Estimation of the Persistence Length of Polymers by MD Simulations on Small Fragments in Solution. Application to Cellulose

Loes M. J. Kroon-Batenburg,*,† Peter H. Kruiskamp,‡ Johannes F. G. Vliegenthart,‡ and Jan Kroon†

Department of Crystal and Structural Chemistry and Department of Bio-Organic Chemistry, Bijvoet Center for Biomolecular Research, Utrecht University, Padualaan 8, 3584 CH Utrecht, The Netherlands

Received: May 29, 1997; In Final Form: August 6, 1997[⊗]

A procedure is described to estimate the persistence length and related properties of a persistent polymer by MD simulations of a small fragment, including solvent effects. The procedure is applied to cellulose in aqueous solution, which leads to an upper limit of the persistence length of 145 ± 10 Å. The occurrence of small amounts of folded conformations seems to be indicated by comparison of the theoretical with experimental data. The behavior of the cellulose chain is consistent with the Kratky−Porod wormlike model.

Introduction

Cellulose and its derivatives show a notable variation in their capacity to form anisotropic solutions dependent on the kind and degree of substitution and on the solvent. The persistence length is strongly related to this capacity. The persistence length of macromolecules is experimentally accessible by, for example, elastic light scattering experiments.[1] In the past many models have been developed to predict the persistence length or related properties such as the characteristic ratio and the radius of gyration.[2−7] These efforts vary in the degree of elaboration but none of them include the effect of the solvent. Recently, Jung et al.[7] discussed the calculation of the persistence length from MD simulations and preferred in vacuo calculations of long molecules (30 repeating units) over time-consuming calculations in solvents. Brant et al.[5] have performed extensive Monte Carlo simulations to create long-chain molecules from dimer in vacuo potential energy surfaces. In our view persistent molecules can be treated on the basis of small repeating units, similar to the approach taken by Brant et al., but by using MD simulations, calculations in solvents become feasible.

In this paper we show that it is relatively straightforward to calculate the persistence length, characteristic ratio, and radius of gyration of cellulose from MD simulations of a small fragment, i.e., cellobiose. The essential difference from previous approaches is that solvent molecules can explicitly be included, thus taking into account the solvent effects. It will be demonstrated that the persistence length is a very sensitive probe to assess flexibility.

Theory

Descriptions of polymer systems start with a model of an ideal macromolecule. The related theory applies to dilute polymer solutions in which no interactions occur between nonbonded segments (i.e., no excluded volume effects). A polymer built up of n repeating units (bonds) with length l in a linear fashion can be characterized by its end-to-end vector $\mathbf{r}$:

$$\mathbf{r} = \sum_{i=1}^{n} \mathbf{l}_i \tag{1}$$

$$r^2 = \sum_{i=1}^{n}\sum_{j=1}^{n} \mathbf{l}_i\mathbf{l}_j$$

$$= nl^2 + 2\sum_{i<j} \mathbf{l}_i\mathbf{l}_j \tag{2}$$

The orientations of the vectors $\mathbf{l}_i$ are subject to fluctuations, and $\mathbf{r}$ shows a distribution of which the moments can be described as an ensemble average, the second moment being

$$\langle r^2\rangle = nl^2 + 2\sum_{i<j}^{n} \langle \mathbf{l}_i\mathbf{l}_j\rangle$$

$$= nl^2 + 2l^2\sum_{i<j}^{n} \langle \cos\theta_{ij}\rangle \tag{3}$$

For a freely jointed chain there are no correlations between the various bond vectors and $\langle \cos\theta_{ij}\rangle = 0$, so $\langle r^2\rangle = nl^2$.

A more realistic model is the freely rotating chain. This model has been developed and extensively described by Benoit, Kratky, Porod, and Flory.[2,8,9] The bonds are linked by a (fixed) valence angle and are thought to freely rotate along a cone (Figure 1). In this case

$$\langle \cos\theta_{ij}\rangle = \langle \cos\gamma\rangle^{j-i} \tag{4}$$

where $j > i$ and γ is the angle between consecutive bonds (i.e. the supplement of the valence angle). For a sufficiently large number of bonds ($|j - i| \gg 1$) this function has the following property:

$$\langle \cos\theta_{ij}\rangle = \exp[-(j - i)l/L_p] \tag{5}$$

where L_p is the persistence length. Using this property and

† Department of Crystal and Structural Chemistry.
‡ Department of Bio-Organic Chemistry.
[⊗] Abstract published in *Advance ACS Abstracts,* September 15, 1997.

S1089-5647(97)01717-3 CCC: $14.00

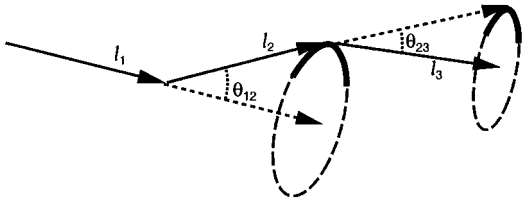

Figure 1. Linking of residues: a (fixed) angle, rotating freely along a cone.

defining the contour length as $L_c = nl$, the following relation is derived:

$$\langle r^2 \rangle = 2L_c L_p - 2L_p{}^2[1 - \exp(-L_c/L_p)] \tag{6}$$

The characteristic ratio

$$C_n = \frac{\langle r^2 \rangle}{nl^2} \tag{7}$$

converges to a specific value C_∞ for each polymer. This value will be unity for the freely jointed chain throughout, but for a stiffer chain with small γ it will be significantly larger. It should be mentioned that the use of C_∞ is not favored because of l^2 in the denominator in eq 1, the value of which is rather arbitrary. However, since it is frequently used in the literature, we also calculate C_∞ in this paper.

The squared radius of gyration is another measure of the size of a macromolecule and is defined as

$$\langle s^2 \rangle = n^{-2} \sum_{1 \le i < j \le n} \langle r_{ij}{}^2 \rangle \tag{8}$$

It is equivalent to the average squared distance of all monomers to the molecule's center of mass. Benoit and Doty[10] have shown that

$$\langle s^2 \rangle = \frac{1}{3} L_c L_p - L_p{}^2 + 2\frac{L_p{}^3}{L_c} - 2\frac{L_p{}^4}{L_c{}^2}[1 - \exp(-L_c/L_p)] \tag{9}$$

For sufficiently long (large L_c) chains $\langle s^2 \rangle = {}^1/_6\langle r^2 \rangle$, and in case of freely rotating chains $\langle s^2 \rangle / nl^2 = {}^1/_6 C_\infty = (1 + \cos\gamma)/(1 - \cos\gamma)$.

Any realistic chain will not be freely rotating, but rather the relative orientations of consecutive bonds are governed by a potential $U(\Psi)$ (Ψ being a parameter that describes this relative orientation), and the distribution of bonds vectors normally only occupies part of the cone, e.g. the black arc in Figure 1. Nevertheless, for larger $j - i$, $\langle \cos\theta_{ij} \rangle$ will behave as a true exponential. The problem in calculating L_p, $\langle r^2 \rangle$, $\langle s^2 \rangle$, and C_∞ then amounts to calculating $\langle \cos\theta_{ij} \rangle$ up to large $j - i$ values, using the proper $U(\Psi)$. This $U(\Psi)$ is determined not only by intramolecular interactions but also by interactions with solvent molecules. This $U(\Psi)$, or rather the probability distribution of Ψ,

$$P(\Psi) = \frac{\exp(-U(\Psi)/kT)}{\int \exp(-U(\Psi)/kT)\, d\Psi} \tag{10}$$

is available from MD simulations, when including solvent molecules explicitly. Kuhn and Kuhn[11] have shown that a wormlike chain can be thought of as segments of length l' that behave like freely jointed chains. This Kuhn length l', which depends on $U(\Psi)$, turns out to be related to the persistence length by $l' = 2L_p$.

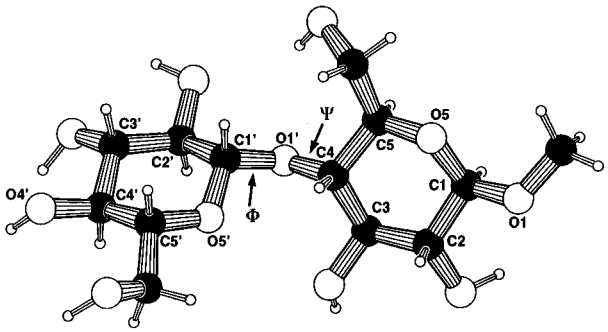

Figure 2. Molecular model of methyl β−D-cellobioside, with relevant atom labels and torsional angles. $\phi = O_5'-C_1'-O_1'-C_4$ and $\psi = C_1'-O_1'-C_4-C_3$.

Method

Several MD simulations of methyl β−D-cellobioside in water have been performed with the program system GROMOS[12] and the standard force field for carbohydrates.[13] The united atom approach is used for aliphatic carbons. The molecule was placed in a truncated octahedral periodic box containing 358 water molecules. For the water molecules the SPC model was used.[14] The simulations were performed at constant temperature (300 K) and pressure with time relaxation constants of 0.1 and 0.5 ps, respectively. All bond lengths were constrained using the SHAKE method.[15] The coordinates of the methyl β−D-cellobioside molecule were stored every 0.2 ps. The first 10 ps of each run was taken as equilibration time. In total the system was simulated for 12 ns. The data at all these time steps represent a statistical mechanical ensemble of configurations $\epsilon(p_1)$, the distribution of which is governed by eq 10. For each of these configurations p_1 ($p_1 = 1...t$ steps) the data were analyzed in the following manner. The monosaccharide repeating units are characterized by vectors $\boldsymbol{l}_1(p_1)$ and $\boldsymbol{l}_2(p_1)$ ($O_4'...O_1'$ and $O_1'...O_1$, respectively, see Figure 2). We thus have a representative set of orientations $\boldsymbol{l}_2$ with respect to $\boldsymbol{l}_1$. The question now is, how would a third monomer ($\boldsymbol{l}_3$) be oriented with respect to the second ($\boldsymbol{l}_2$)? Since the glycosidic linkage 3−2 behaves exactly the same as 2−1, $\boldsymbol{l}_3$ takes the same orientational distribution with respect to $\boldsymbol{l}_2$ as does $\boldsymbol{l}_2$ with respect to $\boldsymbol{l}_1$. The procedure that assigns random orientations for $\boldsymbol{l}_3...\boldsymbol{l}_n$ from the ensemble $\epsilon(p_1)$ is described in the Appendix.

For linkage 2−1 all data points were taken, and for each of these points p_1 the linkage configurations p_k (linkage $(k + 1) - k$) were randomly selected from $\epsilon(p_1)$. This selection is repeated so as to arrive at a desired number of configurations $\epsilon(p_1, p_2, ..., p_3)$. Then following the procedure in the Appendix, $\theta_{i,i+j} = (\boldsymbol{l}_i \boldsymbol{l}_{i+j})/l^2$ can be calculated, and it is straightforward to evaluate $C(j) = \langle \cos\theta_{i,i+j} \rangle$.

Results and Discussion

In a previous paper[16] it has been shown that methyl β−D-cellobioside mainly occupies a single area in (ϕ,ψ) conformational space, i.e., region 1 in Figure 3, while a small amount of conformations in region 3 could not be ruled out completely. Other regions turned out to represent unstable conformations and will no longer be considered. Because conformational transitions between the various regions are slow (nanosecond time scale), they are not easy to sample properly. The more efficient approach in case several regions are occupied is to mix MD trajectories in each of the regions in proper ratios.

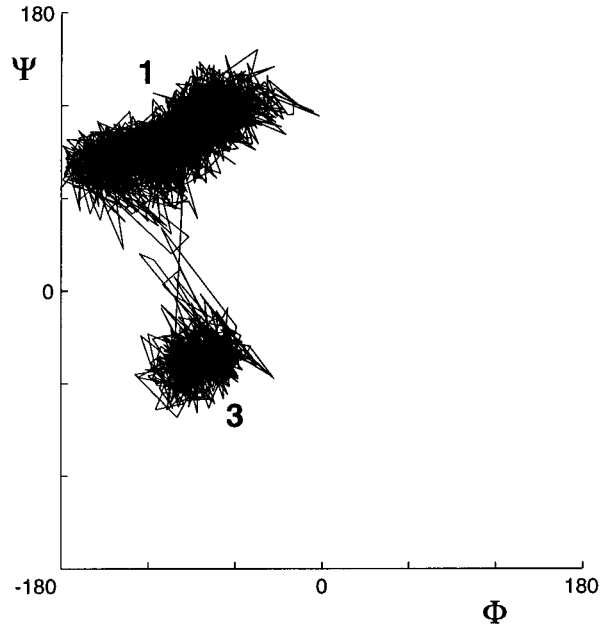

Figure 3. Complete (ϕ,ψ) trajectory used in the analysis.

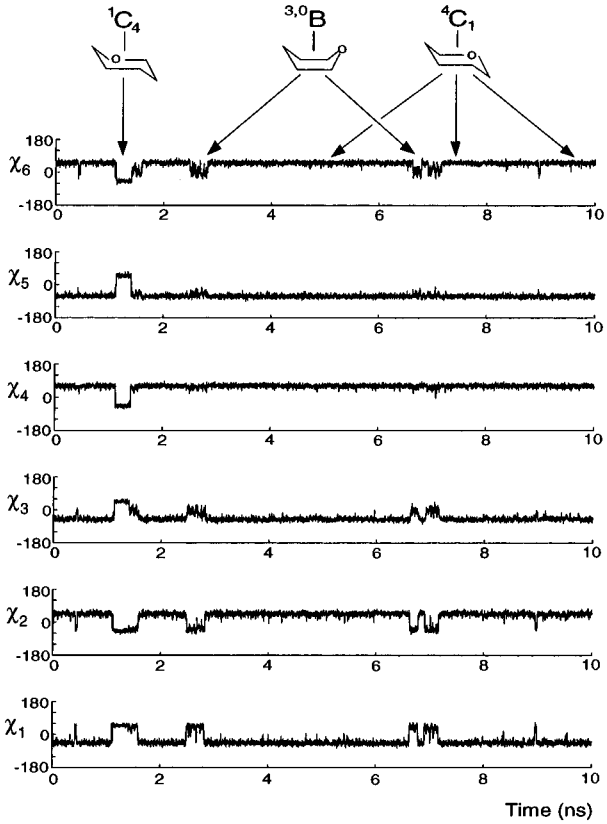

Figure 4. Trajectory showing how the ring torsion angles of first residue change conformation. The torsion angles χ_1, ..., χ_6 are $C_1-C_2-C_3-C_4$, $C_2-C_3-C_4-C_5$, $C_3-C_4-C_5-O_5$, $C_4-C_5-O_5-C_1$, $C_5-O_5-C_1-C_2$, and $O_5-C_1-C_2-C_3$, respectively.

These ratios can be obtained from NMR data. The complete trajectory used in the present analysis is shown in Figure 3.

Occasionally, the usual $^4C_1$ chair conformation converts into a boat or inverted chair conformation. An example of such a trajectory of the six-ring torsion angles of the first ring are given in Figure 4. Mostly the first residue (unprimed residue in Figure 2) displays such a behavior and the ring usually adopts the $^{3,0}B$ boat conformation. The total time spent in such abnormal ring conformations is ~14%. This is more than expected on basis of the analysis of ^3J NMR data of glucose residues in aqueous environment.[17] The total number of transitions is far from sufficient to obtain adequate sampling of the normal versus abnormal ring conformations. In MD simulations, the occurrence of minor species that are occasionally reached by conformational transitions is overestimated because the barrier prohibits immediate retransition. Therefore we decided to divide the trajectory into parts containing normal and abnormal ring conformations, respectively, and to study the influence of increasing amounts of abnormal ring conformations on the persistence length, systematically. Similarly, we have separate trajectories in region 3 (in which no ring inversions happen to occur). We mix these with trajectories in region 1 in controlled amounts.

TABLE 1: Persistence Length, Squared Radius of Gyration, Characteristic Ratio, and End-to-End Distance of Cellulose from MD Simulations in Water[a]

	trajectory region **1**/boat %	L_p	$\langle s^2\rangle$	$\langle s^2\rangle/n$	C_∞	$\langle s^2\rangle^b$
run 1	100/0	145	$574\cdot10^2$	$1.9\cdot10^2$	45	$4068\cdot10^2$
	99/1	131	532	1.8	41	3711
	98/2	119	497	1.7	38	3420
	95/5	98	420	1.4	31	2840
	90/10	73	335	1.1	24	2189
	85/15	65	282	0.9	20	1826
	80/20	52	246	0.8	17	1571
	0/100	75	270	0.9	19	1752
run 2	100/0	147	582	1.9	45	4119
	99/1	134	539	1.8	41	3763
	98/2	124	504	1.7	38	3501
	95/5	99	420	1.4	31	2832
	90/10	75	332	1.1	24	2169
	85/15	60	277	0.9	20	1794
	80/20	51	240	0.8	17	1522
	trajectory region **1**/region **3**	L_p	$\langle s^2\rangle$	$\langle s^2\rangle/$	C_∞	$\langle r^2\rangle^b$
run 1	100/0	145	$574\cdot10^2$	$1.9\cdot10^2$	45	$4068\cdot10^2$
	99/1	122	503	1.7	38	3468
	98/2	105	449	1.5	33	3043
	95/5	77	339	1.1	24	2230
	90/10	51	235	0.8	16	1500
	85/15	37	177	0.6	12	1114
	80/20	30	142	0.5	10	884
	0/100	91	196	0.7	15	1344
run 2	100/0	147	582	1.9	45	4119
	99/1	125	513	1.7	39	3537
	98/2	108	456	1.5	34	3087
	95/5	75	339	1.1	24	2212
	90/10	55	234	0.8	16	1495
	85/15	38	175	0.6	11	1091
	80/20	28	138	0.5	9	851

[a] For chains of 300 residues; $l = 5.51$ Å (average monomer length). [b] L_p in Å, s^2 and r^2 in Å^2.

In Table 1 the results of such a systematic analysis is given. Cellulose chains of 300 residues (bond vectors) have been created using the above procedures. An example of $C(j)$ from a pure region 1 trajectory without abnormal ring conformations is shown in Figure 5. A fit of $C(j)$ to $\exp(-jl/L_p)$ yields the value of L_p of 145 ± 10 Å. A plot of C_n is shown in Figure 6 and approaches a value of C_∞ of 45. The radius of gyration $\langle s^2\rangle^{1/2}$ is 240 Å for 300 residues as calculated by eq 8. A plot of $\langle s^2\rangle/n$ (see Figure 7) shows that for $n = 300$ the value has nearly converged to ~210 Å^2. This implies that $\langle s^2\rangle$ has become linear with n (see Figure 7), consistent with eq 9 for large n. L_p obtained from $\langle s^2\rangle$ via eq 9 is 131 Å. The difference from the above value of L_p is acceptably small given the statistical method by which L_p is estimated. In the coil limit (only using the first part of eq 9) L_p is estimated to be 104 Å. At larger DP (degree of polymerization; typically 400−700 for experimental data) the difference with using the complete eq 9 will be much

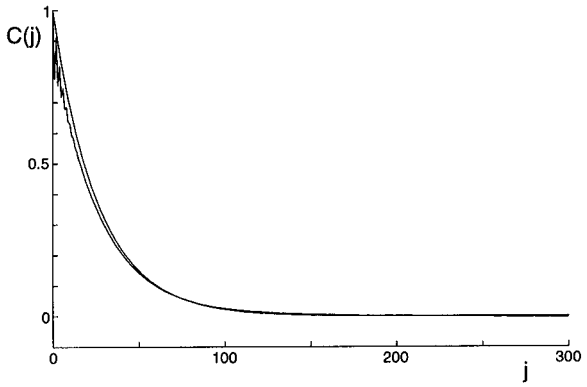

Figure 5. Correlation function $C(j)$ for 300 residues and the exponential curve fitted up to 100 residues.

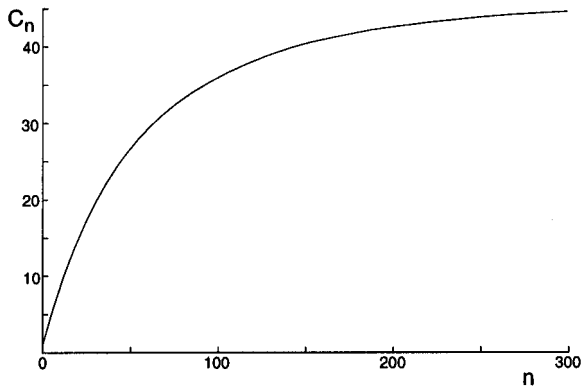

Figure 6. C_n as function of number of residues.

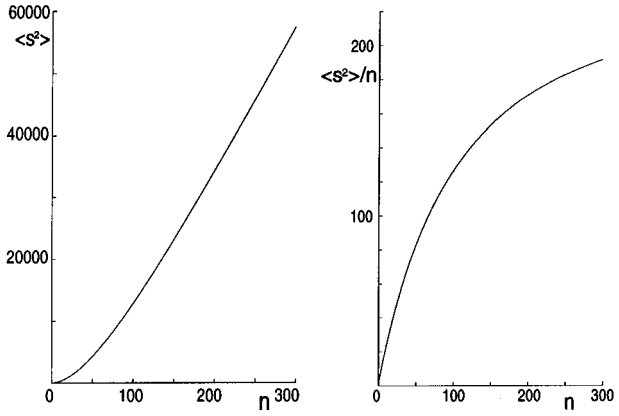

Figure 7. $\langle s^2\rangle$ and $\langle s^2\rangle/n$ in Å^2 as function of number of residues.

reduced. For a freely rotating chain $\langle s^2\rangle_{fr}/n$ would be 13.4 Å^2 ($=^1/_6 l^2(1 + \cos\gamma)/(1 - \cos\gamma)$). This leads to $\sigma^2 \equiv \langle s^2\rangle/\langle s^2\rangle_{fr} = 16.4$, in agreement with the value obtained by Tanner et al.[1] from light-scattering data. This implies that the cellulose chain consists of large persistent stretches that are freely rotating, a situation quite different from a chain with freely rotating monomer residues.

The effect of abnormal ring conformations is shown in Table 1 and Figure 8. It is generally accepted that glucose residues have the $^4C_1$ chair conformation. However, we are not aware of any critical discussion based on ^3J coupling constants from NMR, of what amount of other ring conformations would be compatible with experimental data (i.e., below the detection limit). Since we estimate that the error in measured ^3J coupling constants is approximately 0.1 Hz and in the calculated ^3J values it is 0.5 Hz,[18] this would allow up to 5% of other ring conformations. However, NMR measurements of methyl β−D-glucoside in methanol(d_3)[19] at low temperatures show no transitions to abnormal ring conformations. The chemical shift

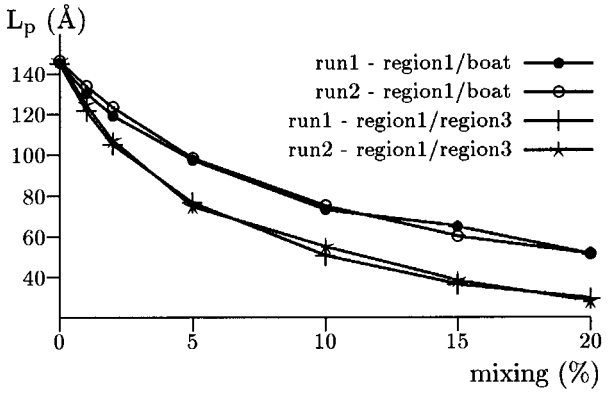

Figure 8. L_p as a function of percentage boat or region 3. 0% referes to the pure region 1 trajectory. Two individual runs of 5 ns in region 1 are used.

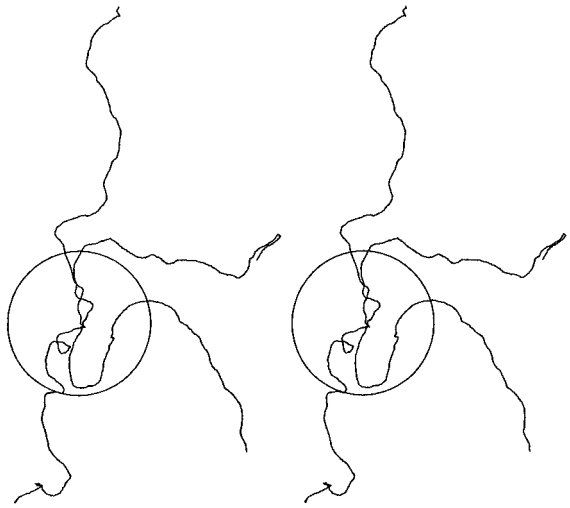

Figure 9. Stereoview of four separate chains built up from conformations in region 1. The radius of the sphere is $\langle s^2\rangle^{1/2} = 240$ Å.

δ_{H1} shows a single signal even at very low T (213 K). If significant amounts of normal and inverted ring conformations would appear, it could be expected to resolve into two signals due to the lower exchange rate. Taking into account the detection limit of the NMR experiments (1%), this would at maximum lead to 3.5% of abnormal ring conformations at 300 K and an energy difference with normal ring conformations of 2 kcal/mol. Ab inito and MM calculations[20,21] indicate that the energy difference between normal and inverted chair or boat conformations should be much larger than that. Therefore we think the occurrence of those conformations will be at maximum 1%, but experimentally this will be hard to prove. In this case the value of L_p would only drop from 145 to 131 Å. In the future a more systematic study of cellulose and derivatives in different solvents will throw some more light on this issue.

Small amounts of the folded conformations in region 3 have a more drastic effect on the L_p and related properties (see Figure 8). Although the recent ROESY−NMR experiments[16] could not unambiguously determine that the methyl cellobioside molecule is exclusively in region 1 in aqueous solution, no more than a few percent of other conformations would be compatible with experiment. Still, this gives an uncertainty in L_p that places it in the range 77−145 Å.

Examples of chain molecules of $n = 300$ in region 1 are depicted in Figure 9. Several observations can be made. First, the molecule indeed behaves like a wormlike chain, with persistent segments that vary in size between 200 and 400 Å, consistent with a Kuhn length that is about twice the persistence length. So even if the molecular conformation is entirely in

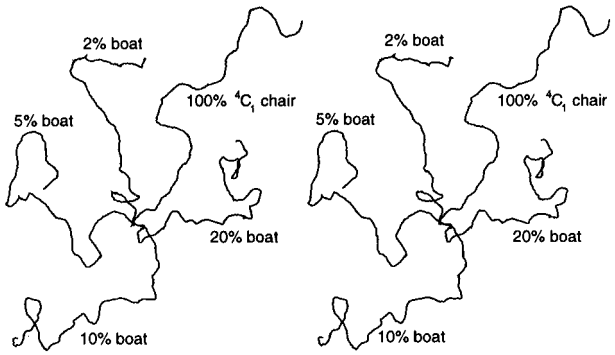

Figure 10. Stereoview of examples of chain molecules ($n = 300$) in region 1 with a percentage of boat structures mixed in.

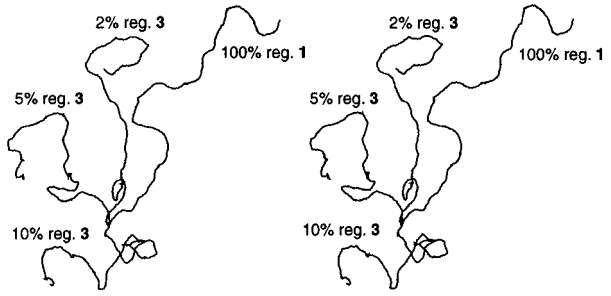

Figure 11. Stereoview of examples of chain molecules ($n = 300$) in region 1 with a percentage of region 3 mixed in.

region 1, it has a wormlike behavior, as was also suggested by Reiling et al.[22] Second, no interactions between remote residues appear to occur. This is caused by the fact that the linkage is largely in the extended conformation. This implies that the assumption that nonbonded monomers do not interact (no excluded-volume interactions) is quite appropriate. Therefore the behavior of cellulose in dilute solutions is completely determined by the behavior of the dimer. Larger amounts of abnormal ring conformations or conformations in region 3 would violate this assumption. This is illustrated in Figures 10 and 11, where chains obtained by mixing with 20% of abnormal ring conformations or 10% conformations in region 3 lead to back-folded structures. However, amounts that are acceptable, as discussed above (5% or less), do not have such an effect.

An overview of the experimental data on physical properties from the literature is given in Table 2. Most of the data concern derivatives of cellulose. From light-scattering and viscosity measurements usually quite different values for the persistence length are found. The radius of gyration is obtained from light scattering and leads to the value of L_p through eq 9 or a simplified form of that. The associated standard deviations are quite large.[23] The L_p obtained through viscosity measurements using the Bohdanecky theory[23,24] tends to be lower and seems more reliable. The L_p range for pure cellulose listed in Table 2 is large: 110−252 Å. Bianchi et al.[23] concluded that the lower limit for pure cellulose using both types of data should be 125 Å. The only measurement in aqueous solution is carried out on hydroxyethyl cellulose, from which a value of ∼90 Å was obtained. Therefore the true value for L_p of our cellulose/water system should be somewhere in the range 90−125 Å. This would indicate that up to 3% of folded conformations (region 3) could occur.

Recently, a discussion on the flexibility of the β 1−4 linkage was given by Hardy et al.[25] A 2D NOESY analysis was performed for methyl α−D-cellobioside. In contrast to what was the case for methyl β−D-cellobioside,[16] no overlap of the $H_1'...H_4$ and $H_1'...H_3/H_5$ NOEs occurred. A small $H_1'...H_3/H_5$ intensity was obtained but could easily be caused by spin diffusion, rather than indicating the existence of conformations in region 3. The authors conclude that occupations of a few percent for the folded conformation could not be ruled out by the experimental data, and as such these data have not yet disproved intrinsic flexibility of the β 1−4 linkage. Previously it was suggested[3,26] that a value of C_∞ of about 35, while simultaneously reproducing the correct temperature coefficient, can only be obtained when twist or boat conformations are taken into account. A similar dependence emerges from our Table 1. However, in view of the above discussion we believe it is more likely that conformations in region 3 are to be held responsible for small C_∞ values. As is clear from Table 2 the standard deviations from the experimentally determined properties are rather large, and only more accurate light-scattering data, viscosity measurements, or NMR experiments can give conclusive evidence. Finally, our calculations were performed in water, a cellulose nonsolvent, whereas none of the experimental data apply to the cellulose/water system. Soon a more extensive comparison of calculated and measured polymer properties will be carried out, by studying derivatives of cellulose in various solvents, where experimental data are present.

It has to be mentioned that nothing in the procedure to build up the chains precludes the generation of back-folded chains, as is demonstrated by the mixtures with region 3 conformations. However, if the number of folded conformations becomes too large, then long-range interactions can no longer be neglected. There could, in reality, be specific long-range interactions that shift the balance to larger amounts of folded conformations, and if their occurrence approaches 10%, this is cause for concern. This will be the subject of future research.

Conclusions

In this paper an approach is described to calculate the persistence length L_p of macromolecules from MD simulations

TABLE 2: Experimental Physical Properties of Cellulose and Derivatives at 25 °C

polymer	solvent	$\langle s^2\rangle/n$ (Å^2)	C_∞	L_p (Å)	ref
cellulose acetate (2.45)	trifluoroethanol	180−235[b]	36−47[c]		1
	methylenechloride−methanol	135−250			1
	tetrahydrofuran	160		95[a]	1
cellulose derivatives (3.0)	various	43−367		70−220[a]	1
cellulose propionate	acetone			70[a]	27
cellulose cyanoethyl−hydroxypropyl	tetrahydrofuran			143[a]	28
cellulose	DMAc/LiCl			110[a] −160[b]	23
cellulose acetate (2.3)	DMAc			70[a]	29
cellulose tris(dimethylphenyl)carbamate	methylpyrrolidone	194[b]		78[b]	30
cellulose	8% NaOH			110[b]	31
cellulose	cuoxam			130[b]	32
cellulose	DMAc/LiCl	331−747[b]	91.9	252[d]	33
hydroxyethyl cellulose	water			88[a] −91[b]	34

[a] Intrinsic viscosity. [b] Light scattering. [c] Assuming $C_\infty = 6\langle s^2\rangle/nl^2$ as for freely rotating chain. [d] Coil limit: $L_p = 3\langle s^2\rangle/nl$.

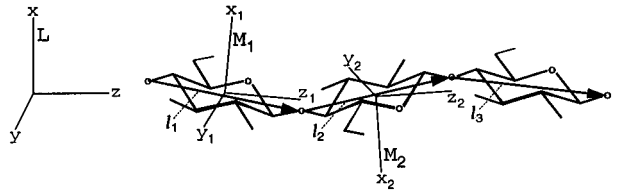

Figure 12. The three axes systems used in the Euler transformations.

of small repeating units, while including the solvent effects explicitly. This leads to good results for persistent (wormlike) molecules, like cellulose. It turns out that the persistence length is very sensitive to small amounts of folded conformations. The range of values for L_p from experimental data and from the uncertainties associated with the theoretical methods is such that small amounts of folded conformations in solvated cellulose cannot be ruled out.

Acknowledgment. This work was supported by The Netherlands Program for Innovation Oriented Carbohydrate Research (IOP-k) with financial aid of the Ministry of Economic Affairs and the Ministry of Agriculture, Nature management and Fisheries and of Akzo Nobel (Arnhem). The authors thank Dr. S. J. Picken and Dr. M. G. Northolt of Akzo Nobel for stimulating discussions and for reading the manuscript.

Appendix

To obtain the distribution of $\mathbf{l_3}$, first the system of axes of inertia, $\mathbf{M}_1$ and $\mathbf{M}_2$, for the two monomers are calculated for each configuration (p_1), as well as the Euler angles that rotate the laboratory axes system $\mathbf{L}$ into $\mathbf{M}_1$ and $\mathbf{M}_2$ (see Figure 12), which are denoted by $\alpha_1(p_1)$, $\beta_1(p_1)$, $\gamma_1(p_1)$ and $\alpha_2(p_1)$, $\beta_2(p_1)$, $\gamma_2(p_1)$. $\mathbf{l}_1$ and $\mathbf{l}_2$ are obtained in $\mathbf{L}$ and will be denoted by $\mathbf{l}_1^{\mathbf{L}}(p_1)$ and $\mathbf{l}_2^{\mathbf{L}}(p_1)$. These are transformed to $\mathbf{l}_1^{\mathbf{M}_1}(p_1)$ and $\mathbf{l}_2^{\mathbf{M}_1}(p_1)$ by the Euler rotation

$$\mathbf{L} \xrightarrow{\alpha_1(p_1),\,\beta_1(p_1),\gamma_1(p_1)} \mathbf{M}_1$$

An essential property is that the distribution of $\mathbf{l}_3^{\mathbf{M}_2}$ is the same as that of $\mathbf{l}_2^{\mathbf{M}_1}$. For any point in the ensemble $\epsilon(p_2)$, which in fact is the same as $\epsilon(p_1)$, $\mathbf{l}_3^{\mathbf{M}_2}(p_2)$ is transformed to the $\mathbf{M}_1$ axes system by

$$\mathbf{l}_3^{\mathbf{M}_2}(p_2) \xrightarrow{-\gamma_2(p_1),\,-\beta_2(p_1),\,-\alpha_2(p_1)} \mathbf{l}_3^{\mathbf{L}}(p_1,p_2) \xrightarrow{\alpha_1(p_1),\,\beta_1(p_1),\,\gamma_1(p_1)} \mathbf{l}_3^{\mathbf{M}_1}(p_1,p_2)$$

The orientation of $\mathbf{l_3}$ is seen to depend on two glycosidic linkage conformations, p_1 for the 2−1 linkage and p_2 for the 3−2 linkage. A similar procedure can be followed for $\mathbf{l}_4^{\mathbf{M}_3}$, which can be transformed to $\mathbf{l}_4^{\mathbf{M}_1}(p_1,p_2,p_3)$. In this way all vectors $\mathbf{l}_n$, with $n > 2$, can be obtained in $\mathbf{M}_1$ by $2(n-2)$ Euler rotations. In $\mathbf{M}_1$ finally $\theta_{i,i+j}$ can be obtained from $(\mathbf{l}_i^{\mathbf{M}_1}\mathbf{l}_{i+j}^{\mathbf{M}_1})/l^2$.

References and Notes

(1) Tanner, D. W.; Berry, G. *J. Polym. Sci.: Polym. Phys.* **1974**, *12*, 941−975.
(2) Benoit, H. *J. Polym. Sci.* **1948**, *3*, 376−388.
(3) Brant, D. A.; Goebel, K. D. *Macromolecules* **1972**, *5*, 536−538.
(4) Brant, D. A. *Carbohydr. Polym.* **1982**, *2*, 232−237.
(5) Brant, D. A.; Christ, M. D. *ACS Symposium Series*; Washington, DC, 1990; Vol. 430, Chapter 4.
(6) Jung, B.; Schürmann, B. L. *Makromol. Chem. Rapid Commun.* **1989**, *10*, 419−425.
(7) Jung, B.; Schürmann, B. L. *Macromolecules* **1989**, *22*, 477−480.
(8) Kratky, O.; Porod, G. *Recl. Trav. Chim. Pays-Bas.* **1949**, *68*, 1106−1122.
(9) Flory, P. J. *Statististical Mechanics of Chain Molecules*; Interscience: New York, 1969.
(10) Benoit, H.; Doty, P. *J. Chem. Phys.* **1953**, *57*, 958−963.
(11) Kuhn, W.; Kuhn, H. *Helv. Chim. Acta* **1943**, *26*, 1394−1465.
(12) van Gunsteren, W. F. *Gromos*, Groningen molecular simulation package; University of Groningen, 1987.
(13) Koehler, J.; Saenger, W.; van Gunsteren, W. F. *Eur. Biophys. J.* **1987**, *15*, 197−210.
(14) Berendsen, H. J. C.; Postma, J. P.; van Gunsteren, W. F.; Hermans, J. 1981; Reidel Publishing: Dordrecht, The Netherlands, pp 331−342.
(15) Gunsteren, W. F.; Berendsen, H. J. C. *Mol. Phys.* **1977**, *34*, 1311−1327.
(16) Kroon-Batenburg, L. M. J.; Kroon, J.; Leeflang, B. R.; Vliegenthart, J. F. G. *Carbohydr. Res.* **1993**, *245*, 21−42.
(17) Lemieux, R. U. *Can. J. Chem.* **1966**, *44*, 249−262.
(18) Haasnoot, C. A. G.; de Leeuw, F. A. A. M.; Altona, C. *Tetrahedron* **1980**, *36*, 2783−2792.
(19) Kruiskamp, P. H. Unpublished results.
(20) Barrows, S.; Dulles, F.; Cramer, C.; French, A.; Truhlar, D. *Carbohydr. Res.* **1995**, *276*, 219−251.
(21) Dowd, M. K.; French, A. D.; Reilly, P. J. *Carbohydr. Res.* **1994**, *264*, 1−19.
(22) Reiling, S.; Brickmann, J. *Macrmol. Theory Simul.* **1995**, *4*, 725−743.
(23) Bianchi, E.; Ciferri, A.; Conio, G.; Cosani, A.; Terbojevich, M. *Macromolecules* **1985**, *18*, 646−650.
(24) Bohdanecky, M. *Macromolecules* **1983**, *16*, 1483−1492.
(25) Hardy, B. J.; Gutierrez, A.; Lesiak, K.; Seidl, E.; Wildmalm, G. *J. Phys. Chem.* **1996**, *100*, 9187−9192.
(26) Goebel, K. D.; Brant, D. A. *Appl. Polym. Symp.* **1976**, *28*, 671−691.
(27) Casay, G. A.; George, A.; Hadjichristidis, N.; Lindner, J. S.; Mays, J. W.; Peiffer, D. G.; Wilson, W. W. *J. Polym. Sci.: Polym. Phys.* **1995**, *33*, 1537−1544.
(28) Mays, J. W. *Macromolecules* **1988**, *21*, 3179−3183.
(29) Bianchi, E.; Ciferri, A.; Conio, G.; Lanzavecchia, L.; Terbojevich, M. *Macromolecules* **1986**, *19*, 630−636.
(30) Tsuboi, A.; Norisuye, T.; Teramoto, A. *Macromolecules* **1996**, *29*, 3597−3602.
(31) Kamide, K.; Saito, M.; Kowasa, K. *Polym. J.* **1987**, *19*, 1173.
(32) Burchard, W.; Habermann, N.; Klüfers, P.; Seger, B.; Wilhelm, U. *Angew. Chem., Int. Ed. Engl.* **1994**, *33*, 884−887.
(33) McCormick, C. L.; Callais, P. A.; Hutchinson, B. H., Jr. *Macromolecules* **1985**, *18*, 2394−2401.
(34) Brown, W. *Arkiv Kemi.* **1962**, *18*, 227−284.